

This is a repository copy of *Impact of surface ozone interactions on indoor air chemistry:a modelling study*.

White Rose Research Online URL for this paper:

<https://eprints.whiterose.ac.uk/id/eprint/114878/>

Version: Published Version

---

**Article:**

Kruza, M., Lewis, A. C. [orcid.org/0000-0002-4075-3651](https://orcid.org/0000-0002-4075-3651), Morrison, G. C. et al. (1 more author) (2017) Impact of surface ozone interactions on indoor air chemistry:a modelling study. *Indoor air*. 10.1111/ina.12381. pp. 1001-1011. ISSN: 0905-6947

<https://doi.org/10.1111/ina.12381>

---

**Reuse**

This article is distributed under the terms of the Creative Commons Attribution (CC BY) licence. This licence allows you to distribute, remix, tweak, and build upon the work, even commercially, as long as you credit the authors for the original work. More information and the full terms of the licence here:

<https://creativecommons.org/licenses/>

**Takedown**

If you consider content in White Rose Research Online to be in breach of UK law, please notify us by emailing [eprints@whiterose.ac.uk](mailto:eprints@whiterose.ac.uk) including the URL of the record and the reason for the withdrawal request.

## ORIGINAL ARTICLE

# Impact of surface ozone interactions on indoor air chemistry: A modeling study

M. Kruza<sup>1</sup> | A. C. Lewis<sup>2</sup> | G. C. Morrison<sup>3</sup>  | N. Carslaw<sup>1</sup> <sup>1</sup>Environment Department, University of York, York, UK<sup>2</sup>Wolfson Atmospheric Chemistry Laboratories, Department of Chemistry, University of York, York, UK<sup>3</sup>Department of Civil, Architectural, and Environmental Engineering, Missouri University of Science and Technology, Rolla, MO, USA**Correspondence**Nicola Carslaw, Environment Department, University of York, York, UK.  
Email: nicola.carslaw@york.ac.uk**Funding information**

The European Union's Seventh Framework Programme

**Abstract**

An INdoor air Detailed Chemical Model was developed to investigate the impact of ozone reactions with indoor surfaces (including occupants), on indoor air chemistry in simulated apartments subject to ambient air pollution. The results are consistent with experimental studies showing that approximately 80% of ozone indoors is lost through deposition to surfaces. The human body removes ozone most effectively from indoor air per square meter of surface, but the most significant surfaces for C<sub>6</sub>-C<sub>10</sub> aldehyde formation are soft furniture and painted walls owing to their large internal surfaces. Mixing ratios of between 8 and 11 ppb of C<sub>6</sub>-C<sub>10</sub> aldehydes are predicted to form in apartments in various locations in summer, the highest values are when ozone concentrations are enhanced outdoors. The most important aldehyde formed indoors is predicted to be nonanal (5-7 ppb), driven by oxidation-derived emissions from painted walls. In addition, ozone-derived emissions from human skin were estimated for a small bedroom at nighttime with concentrations of nonanal, decanal, and 4-oxopentanal predicted to be 0.5, 0.7, and 0.7 ppb, respectively. A detailed chemical analysis shows that ozone-derived surface aldehyde emissions from materials and people change chemical processing indoors, through enhanced formation of nitrated organic compounds and decreased levels of oxidants.

**KEYWORDS**C<sub>6</sub>-C<sub>10</sub> aldehydes, indoor air quality, nitrated organic species, ozone deposition, skin emissions, surface chemistry

## 1 | INTRODUCTION

Many sources contribute to indoor air pollution. Indoor contaminants can originate outdoors (ie, ozone [O<sub>3</sub>], nitrogen oxide [NO<sub>x</sub>], particulate matter [PM]); however, there are also significant sources indoors.<sup>1</sup> The main indoor air pollutant sources are indoor activities such as cooking (eg, NO<sub>x</sub>, PM),<sup>2</sup> smoking (such as formaldehyde [HCHO], PM)<sup>3</sup> or cleaning (eg, terpenes).<sup>4</sup> An increasingly active area of research for indoor air pollution is that driven by emissions from internal materials such as carpets, painted walls, or furniture.<sup>5-7</sup>

Species can be emitted directly from a surface (primary pollutants), but also following gas-phase transformations or interactions at surfaces (secondary pollutants) as shown in Figure 1. Furthermore, these processes form an effective means of removing air pollutants prone to deposition, that is, ozone, from indoor air, and consequently, the concentrations of these species are much lower indoors than outdoors.<sup>8</sup>

Surface deposition depends on two main processes: the transport of ozone to the surface and the uptake to the surface. Transport to the surface is determined by the thickness of the surface boundary layer.<sup>9</sup> The rate of ozone that is removed from indoor air (ozone loss)

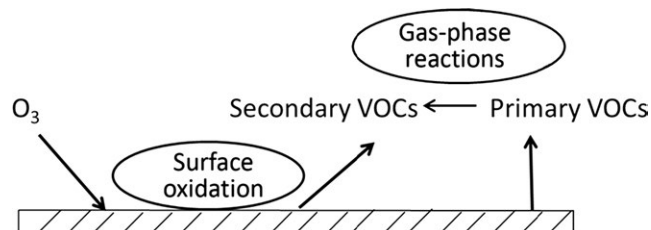


**FIGURE 1** Primary and secondary VOC formation following surface deposition of ozone through oxidation processes and gas-phase transformations

is proportional to the indoor ozone concentration, air exchange rate, surface area with a characteristic deposition velocity different for each surface material and a total volume of indoor space.<sup>10</sup> Indoor surfaces range from highly reactive (carpet) to poorly reactive (glass). The deposition rate for materials like carpet is mostly limited by external mass transport, while deposition to glass is typically limited by surface reaction kinetics.

Ozone is one of the most reactive compounds indoors and in the absence of indoor sources mostly originates outdoors.<sup>11</sup> Once indoors, it can undergo a number of loss processes depending on the conditions, but deposition usually dominates. Porous and fleecy surfaces, such as carpets and soft furniture, are important sinks of ozone and are also able to form a wide range of higher ( $C_6$  and above) aldehydes.<sup>12</sup> The age of the material is also significant because emission rates tend to be higher for new materials and reduce as a material becomes older.<sup>13,14</sup> Morrison and Nazaroff<sup>15</sup> termed this process “ozone aging.” Ozone can oxidize the available unsaturated bonds in a surface coating over time, leading to decreasing ozone uptake and also decreasing emission rates of secondary pollutants from this source.

There is a significant difference between the temporal evolution of primary and secondary pollutants indoors. Emission of primary VOCs tends to decline at a predictable rate and generally reduces to lower levels within a year.<sup>16,17</sup> The formation rate of secondary pollutants is more prolonged, as ozone uptake and consequent surface processing to produce secondary pollutants can continue for several years.<sup>14</sup> Products of these reactions include aldehydes and ketones<sup>8,18</sup> and secondary organic aerosols (SOA).<sup>19</sup> Furthermore, secondary pollutants from surface production can be more damaging for human health than the primary emissions, causing asthma and pulmonary infections<sup>20</sup> and thus warrant further investigation.

One surface receiving increasing attention indoors is the human body. Humans are an important sink for ozone in the indoor environment. The chemicals that constitute human skin can be classified as wax esters, glycerols, fatty acids, squalene, esters, and sterols and contain unsaturated carbon bonds which readily react with ozone.<sup>21</sup> Following such reactions, a wide range of secondary products can be formed, including aldehydes, ketones, acids, and SOA, some of which are known to be harmful to health.<sup>22,23</sup>

In the absence of comprehensive indoor air measurements, indoor air pollutant concentrations can be simulated using a detailed indoor air chemistry model. Such models can provide insight into mechanisms

### Practical Implications

- This article investigates secondary pollutant formation following surface interactions indoors. The concentrations of several aldehyde species can reach appreciable concentrations indoors, particularly when outdoor ozone concentrations are enhanced such as during clear-sky high-pressure conditions. This is a concern, as there is the potential for an increased frequency of polluted episodes associated with blocking anticyclones in the future as the climate warms. Further, some aldehyde species have known or suspected adverse health effects. Finally, the presence of surface emissions following deposition indoors is shown to enhance the formation of nitrated organic species, a further class with potential toxicological effects.

that influence chemical processing, which is essential to understand the fundamental science and hence apply appropriate mitigation strategies. The aim of this study is to develop an existing model to include ozone-derived surface emissions and probe the implications of these emissions on indoor air composition. In particular, ozone deposition onto surfaces and resultant secondary pollutant formation in a simulated apartment is investigated. Different surface types are considered, such as soft furniture, painted wall, hard furniture, wooden floor, linoleum, countertop, and human skin. We quantify secondary pollutant concentrations generated from ozone reactions with these surfaces, as well as use the model to investigate the impact of ozone-initiated surface emissions on chemical processing and pathways in indoor air.

## 2 | METHODOLOGY

### 2.1 | Model development

An Indoor air Detailed Chemical Model (INDCM) has been developed based on previous work by Carslaw<sup>24</sup> and Carslaw et al.<sup>25</sup> The INDCM uses a comprehensive chemical mechanism called the Master Chemical Mechanism, MCM v3.2 (<http://mcm.leeds.ac.uk/MCM/>) and considers the chemical breakdown of 143 VOCs indoors.<sup>26,27</sup> The degradation process of VOCs is initiated by reactions with OH,  $O_3$ ,  $NO_3$ , and photolysis where relevant. Radicals are generated as intermediate products, such as oxy (RO) and peroxy ( $RO_2$ ) radicals, excited, and stabilized Criegee ( $R'R''COO$ ) species, which can undergo a number of further reactions. A range of products such as alcohols, carbonyls, and nitrates are formed, until carbon dioxide and water are produced. The MCM also includes an inorganic scheme including reactions of ozone,  $NO_x$ , and carbon monoxide.<sup>26–29</sup> The INDCM includes approximately 20 000 gas-phase chemical and photolysis reactions, as well as a representation of indoor-outdoor exchange, VOC emissions, surface deposition, and gas to particle formation for limonene.<sup>25</sup>

The INDCM considers a single well-mixed environment and assumes that the concentration of each species is calculated according to Equation 1<sup>25</sup>:

$$\frac{dC_i}{dt} = -v_d \left( \frac{A}{V_i} \right) C_i + \lambda_r f C_o - \lambda_r C_i + \frac{E_i}{V_i} + \sum_{j=1}^n R_{ij} \quad (1)$$

where  $C_i$  ( $C_o$ ) is the indoor (outdoor) concentration of species,  $v_d$  its deposition velocity,  $A$  the surface area indoors,  $V_i$  the volume of air in the indoor environment,  $\lambda_r$  the air exchange rate between indoors and outdoors (AER),  $f$  the building filtration factor,  $E_i$  the indoor emission rate for species  $i$ , and  $R_{ij}$  the reaction rate between species  $i$  and  $j$ .

For this study, the INDCM has been developed to consider ozone deposition onto different types of surface, as well as emissions of higher aldehydes following surface interaction. The ozone loss rate to a surface is calculated according to Equation 2:

$$F_{s1...n} = v_{dO_3} \frac{A_s}{V_i} \quad (2)$$

where  $F_{s1...n}$  is the ozone deposition flux to the surface from 1 to  $n$  number of surfaces,  $v_{dO_3}$  is the ozone deposition velocity to a surface,  $A_s$  is the surface area (total area of a specific surface type),  $V_i$  is the total volume of the indoor environment.

The emission of the surface products was calculated using Equation 3<sup>30</sup>:

$$E_{sec,1...n} = \frac{A_s Y C_{O_3} v_{dO_3}}{V_i} \quad (3)$$

where  $E_{sec,1...n}$  is the relevant secondary product emission rate from 1 to  $n$  number of surfaces,  $Y$  is the aldehyde yield of the emitted pollutant, and  $C_{O_3}$  is the bulk ozone concentration.

## 2.2 | Ozone deposition velocity

The uptake of ozone from indoor air is different for each type of surface, characterized by a specific deposition velocity.<sup>31</sup> Accordingly, based on a review of published measurements,<sup>31–33</sup> characteristic deposition velocities for ozone on different types of materials were defined in terms of maximum, median, and minimum values.

Figure 2 shows that relatively large differences in the ozone deposition velocity exist both within and between surface types. The differences likely arise due to differences in measurement techniques, experimental conditions (eg, near-surface air velocities), and the duration of the measurements. Moreover, differences in ozone deposition velocity within the same type of material are subject to the chemical composition of the surface coating, its gas permeability, the type, and the porosity of the substrate material, as well as the presence of a film on the surface.<sup>31,32,41,42</sup> For instance, painted wood materials are characterized by 2–5 times larger values of ozone deposition velocities than the values on oiled or lacquered wood materials.<sup>32</sup> Lin and Hsu<sup>12</sup> noted that fleecy and spongy materials can be described by higher deposition velocities than plane and smooth surfaces. Finally, Abbass et al.<sup>43</sup> noted that the fiber material used within carpets had a large effect on both ozone deposition and also subsequent oxidation-derived

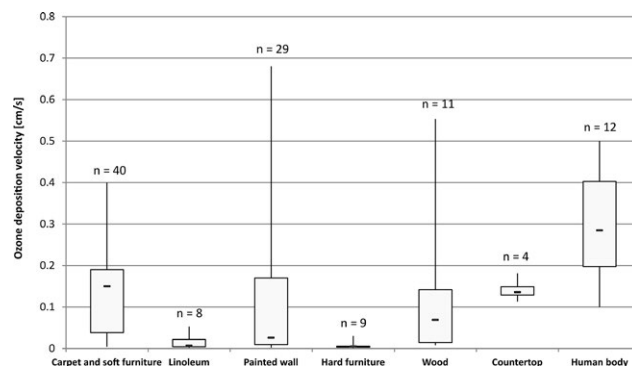


**FIGURE 2** Distribution of reported ozone deposition velocity onto different indoor surfaces, considering number of measurements ( $n$ ) for each. The box and whisker plot shows the minimum, 25%, median, 75% and maximum values in  $\text{cm s}^{-1}$ . 5,9,12,14,15,21,31–40

aldehyde emissions. Consequently, we considered a range of values when carrying out the model runs.

## 2.3 | Surface production of $C_6$ – $C_{10}$ aldehydes

Hexanal, heptanal, octanal, nonanal, and decanal are the carbonyls generated with the highest yields<sup>14</sup> as secondary pollutants from building surfaces. Although lower molecular weight carbonyl species are also emitted from surfaces, far less data are available. Degradation mechanisms were absent in the MCM for octanal, nonanal, and decanal, so new schemes have been developed based on analogy with the existing heptanal scheme. The reaction rate coefficients for OH with higher aldehydes were taken from the literature, with  $3.2 \times 10^{-11} \text{ cm}^3 \text{ mol}^{-1} \text{ s}^{-1}$  used for octanal,<sup>44</sup>  $3.6 \times 10^{-11} \text{ cm}^3 \text{ mol}^{-1} \text{ s}^{-1}$  for nonanal<sup>45</sup>, and  $3.6 \times 10^{-11} \text{ cm}^3 \text{ mol}^{-1} \text{ s}^{-1}$  was also assumed for decanal, based on the literature values for nonanal and undecanal both being this value.<sup>44,45</sup> The background indoor concentrations of the aldehyde species arise from primary emissions, indoor-outdoor exchange, and, in some cases, additional gas-phase chemistry. Outdoor concentrations were based on Hodgson et al.<sup>18</sup>

Wang and Morrison<sup>14</sup> measured aldehyde yields for different surfaces following uptake of ozone in four homes, calculated as a summer and a winter average as well as yields from two new (1 and 2 years old) and from two old (12 and 14 years old) homes in summer time. To calculate the oxidation-derived emissions of higher aldehydes from surfaces as defined in the Model development section (Section 2.1), we have used aldehyde yields. Table 1 shows aldehyde yields in summer from new and old surfaces and also calculated as an average of the two. New surfaces typically have higher yields than older ones, with the exception of painted walls although few results exist for this surface. Table 1 also includes product yields of various species following human body-ozone interactions measured in an aircraft cabin.<sup>22</sup> The products detected comprised unsaturated aliphatic aldehydes, ketones, and carboxylic acids, so we have included in our study those aldehydes that are already represented in our model: nonanal, decanal, and 4-oxopentanal (4-OPA).

**TABLE 1** Aldehyde yields (calculated as average values adopted from measurements data) in summer for average age, new, and old surface type<sup>38</sup> and average yields from human body emissions with a stated uncertainty of 15%-25%.<sup>22</sup> Note that figures are rounded to two significant figures

Surface type	Compound	No. of measurements (n)	Average age surface aldehyde yield (±SD)	New surface aldehyde yield	Old surface aldehyde yield
Carpet and soft furniture	Hexanal	16	0.03 (±0.03)	0.03	0.03
	Heptanal		0.01 (±0.01)	0.01	0.00
	Octanal		0.01 (±0.02)	0.01	0.01
	Nonanal		0.06 (±0.03)	0.08	0.04
	Decanal		0.03 (±0.03)	0.04	0.02
Painted wall	Octanal	3	0.01 (±0.02)	0.00	0.03
	Nonanal		0.13 (±0.18)	0.03	0.34
	Decanal		0.04 (±0.07)	0.01	0.12
Countertop	Hexanal	12	0.08 (±0.05)	0.09	0.06
	Heptanal		0.02 (±0.02)	0.03	0.02
	Octanal		0.01 (±0.01)	0.01	0.02
	Nonanal		0.26 (±0.15)	0.33	0.19
	Decanal		0.03 (±0.04)	0.04	0.03
Linoleum	Hexanal	7	0.07 (±0.06)	0.08	0.06
	Heptanal		0.01 (±0.01)	0.01	0.00
	Octanal		0.01 (±0.02)	0.02	0.01
	Nonanal		0.13 (±0.10)	0.20	0.04
	Decanal		0.03 (±0.04)	0.05	0.00
Human body <sup>1</sup>	Nonanal	4	0.018	–	–
	Decanal		0.026	–	–
	4-OPA		0.026	–	–

<sup>1</sup>Note that the yields of decanal and 4-OPA reported by Weschler et al.<sup>22</sup> derive almost exclusively from ozone-skin oil chemistry, but the yield of nonanal has been halved to reflect the fact that emissions from internal surfaces were also included in the yield estimates (Professor Charles J. Weschler, EOHHS, Rutgers University, NJ, USA, personal communication).

As the data for aldehyde yields for wooden materials were not available, direct emission rates were calculated using literature data for different types of wooden materials.<sup>33</sup>

## 2.4 | Base case scenario

We consider an apartment in Milan for this modeling study, using typical and heatwave summer conditions.<sup>46</sup> Milan is a highly polluted city due to traffic emissions and poor dispersion.<sup>47</sup> Summer ozone concentrations are often high in Milan, but during the heat wave that occurred in Europe in summer 2003, concentrations were exceptionally

high for several days (Table 2). Given that high outdoor ozone concentrations lead to high indoor ozone concentrations, Milan was considered a good study site for reactive indoor chemistry as shown through previous studies.<sup>46,48</sup> However, we also considered more typical summertime conditions through an identical apartment in Seoul, which has much lower outdoor ozone concentrations in summer (Table 2). Note that Seoul is a study location as part of the CAPACITIE project,<sup>49</sup> which provided funding for this study.

We assumed a typical apartment size using data proposed by Tae et al.<sup>50</sup> The apartment has three bedrooms each of 7.5 m<sup>2</sup> with an open-plan kitchen/living room 12.5 and 20.9 m<sup>2</sup>, respectively, a small

**TABLE 2** Outdoor and indoor concentrations of ozone, NO<sub>2</sub>, and NO measured and predicted as an average (09:00-17:00 hours) for the heat-wave period of 2 weeks in August 2003 and the same 2 weeks in August 2009 in the Milan apartment and the averages from June to August 2012-2014 for the apartment in Seoul

	Ozone outdoors (ppb)	NO <sub>2</sub> outdoors (ppb)	NO outdoors (ppb)	Ozone indoors (ppb)	NO <sub>2</sub> indoors (ppb)	NO indoors (ppb)
Milan 2003	75.2	30.5	14.1	15.1	10.4	0.6
Milan 2009	49.0	19.1	16.0	9.2	8.2	1.1
Seoul	34.4	25.0	9.2	7.2	7.9	0.8

toilet (2.8 m<sup>2</sup>), bathroom (7.8 m<sup>2</sup>), corridor (3.9 m<sup>2</sup>), and ceiling height of 2.4 m, giving a total surface area of 70 m<sup>2</sup> and a volume of 168 m<sup>3</sup>.

The surface to volume ratio (HMIX) is determined by the indoor dimensions, surface coverings, and furnishing. The apartment is assumed to contain different types of surface found in a typical home<sup>51,52</sup> such as hard furniture together with internal doors (22 m<sup>2</sup>; HMIX=0.13 m<sup>-1</sup>), soft furniture (35 m<sup>2</sup>; HMIX=0.21), wooden floors (51 m<sup>2</sup>; HMIX=0.30 m<sup>-1</sup>), painted walls and ceilings (199 m<sup>2</sup>; HMIX=1.18), linoleum including the kitchen, bathroom, and toilet floors (11 m<sup>2</sup>; HMIX=0.07) and countertops, including those in the kitchen, toilet, and bathroom and tiled toilet, bathroom, and kitchen walls (19 m<sup>2</sup>; HMIX=0.11). This gives a total surface area for deposition of 337 m<sup>2</sup> (HMIX=2.0 m<sup>-1</sup>). Thus, it is possible to compare different types of surfaces that have different sorption properties and ozone removal rates.<sup>41</sup>

Furthermore, to evaluate the importance of human bodies for ozone loss and indoor surface interactions, it was assumed that two adults and one child were in the household. The surface area of a human body was estimated as 2 m<sup>2</sup> for adults and 1 m<sup>2</sup> for children (in total HMIX for skin is ~0.03 m<sup>-1</sup>).<sup>10</sup> Thus, the total surface area available for surface interactions, including the presence of people, amounts to 342 m<sup>2</sup> and the total surface to volume ratio for the building is ~2.0 m<sup>-1</sup>.

## 2.5 | Indoor-outdoor air exchange rate (AER)

Based on statistical analysis of data from approximately 2000 households, the baseline air exchange rate (AER) was assumed to be 0.76 per hour,<sup>53</sup> although AER extremes of 0.2 and 2.0 per hour<sup>11</sup> are examined to evaluate the impact of different ventilation conditions. This range also incorporates the likely range of values for European apartments.<sup>54</sup> An AER of 0.2 per hour is considered as a representative value for tightly constructed, energy-efficient housing whereas an AER of 2.0 per hour is more typical for more loosely constructed building.<sup>25</sup>

## 2.6 | Initial concentrations

The mean outdoor Milan concentrations of ozone, NO<sub>2</sub>, and NO during 2 weeks in August 2003 and the same 2 weeks in a typical summer in 2009 have been taken from the EU AirBase<sup>55</sup> data set.<sup>48</sup> Typical outdoor concentrations for Seoul were taken from the summer time period (June, July, August) of 3 years (2012-2014; Professor Kyungho Choi, Seoul National University, South Korea, personal communication). Outdoor VOC concentrations were available from the EU OFFICAIR project<sup>56</sup> or set to typical outdoor values in an urban area<sup>48,57</sup> and assumed the same in both cities. For C<sub>6</sub>-C<sub>10</sub> aldehydes, outdoor values of hexanal, heptanal, octanal, nonanal, and decanal were assumed constant at 0.37, 0.15, 0.29, 1.0, and 0.11 ppb, respectively, for each location based on measurements outside US houses in residential areas.<sup>18</sup> We return to these assumptions in Section 3.3, but highlight the relative paucity of such measurements in the literature.

Indoor VOC concentrations were taken from Sarwar et al.<sup>57</sup> or Zhu et al.<sup>58</sup> Outdoor measured O<sub>3</sub> and NO<sub>x</sub> concentrations are presented in Table 2, along with the indoor modeled concentrations for comparison.

## 2.7 | Photolysis

Outdoor photolysis rates were calculated following the method described in detail by Carslaw.<sup>24</sup> Basically, a two-stream isotropic scattering model uses the longitude, latitude, time of year, and day to calculate location and time specific clear-sky photolysis rates.<sup>26</sup> Such values must then be attenuated to be representative for indoors. Although there is limited information in the literature, recent measurements<sup>59</sup> have shown that while light at the visible wavelengths needed to photolyze NO<sub>2</sub> and HONO is typically attenuated to 10%-15% of that outdoors, for species photolyzed in the UV (such as ozone to give excited oxygen state atoms), transmission is typically <1% of that outdoors. Nazaroff and Cass<sup>60</sup> found that 0.7% and 0.15% of visible and UV light, respectively, were transmitted through museum skylights and 0.15% in the UV, while for two laboratories in Greece with large windows, 70%-80% of the visible light was transmitted indoors compared to 25%-30% in the UV.<sup>42</sup> Values of 10% and 3%, respectively, for transmission of visible and UV light are assumed for the baseline model,<sup>24</sup> but the sensitivity of the model to this assumption is tested in Section 3.1. Indoor temperature was assumed to be 27°C and RH 45%.<sup>48</sup>

# 3 | RESULTS AND DISCUSSION

## 3.1 | Model sensitivity analysis

Given the large uncertainty ranges in the input parameters, a series of sensitivity tests have been carried out to investigate the effect of changing key parameters on the predicted concentrations of C<sub>6</sub>-C<sub>10</sub> aldehydes. We either varied key parameters within uncertainty limits (eg, rate coefficients) or varied them within a typical observed range. Transmission of outdoor UV and visible light through the windows was varied between 0.15% and 25% for UV light and between 0.7% and 75% for visible light.<sup>24</sup> Ozone deposition velocities were varied such that all values were set to the 25 percentile or the 75 percentile values of the range reported in the literature as indicated in Section 2.2. Selected rate coefficients were varied to the maximum values of their uncertainty range according to IUPAC<sup>61</sup> as per the method reported by Carslaw et al.<sup>62</sup> Key outdoor concentrations of ozone, NO<sub>x</sub>, and HMIX values were either increased or decreased by 50%, and we investigated the effect of using the aldehyde yields for new and old materials instead of the average yields. The concentrations of the C<sub>6</sub>-C<sub>10</sub> aldehydes were then investigated between 09:00 and 17:00 hours for the conditions described earlier in the Methods section. The results from the sensitivity analysis are shown in Table 3.

The model predictions are sensitive to a number of factors, particularly changes in deposition velocities, photolysis rates, outdoor ozone concentration, and the age of the materials considered. Uncertainties

Scenario	Hexanal	Heptanal	Octanal	Nonanal	Decanal
UV=0.15%, VIS=0.7%	-4.9	-4.8	-4.7	-5.6	-6.0
UV=25%, VIS=75%	30.0	29.6	29.1	34.1	36.4
$\nu_d$ 25‰	-36.9	-17.8	-31.6	-21.4	-34.2
$\nu_d$ 75‰	-29.0	-36.2	15.5	38.1	50.5
OH+Nonanal*1.19	-0.1	-0.1	-0.1	-0.6	0.1
Outdoor $O_3$ *0.5	-53.5	-48.0	-46.8	-52.7	-55.2
Outdoor $O_3$ *1.5	55.8	50.1	48.9	55.0	57.6
Outdoor $NO_x$ *0.5	15.5	14.0	13.7	15.5	16.2
Outdoor $NO_x$ *1.5	-16.5	-14.9	-14.6	-16.4	-17.2
Outdoor $C_6-C_{10}$ *0.5	-3.3	-7.9	-8.9	-3.7	-1.5
Outdoor $C_6-C_{10}$ *1.5	3.3	8.0	9.0	3.7	1.5
HMIX*0.5	5.2	9.9	10.4	7.4	7.4
HMIX*1.5	-11.1	-10.4	-10.3	-8.1	-7.4
Old materials	10.2	-18.7	10.5	5.0	6.3
New materials	-5.9	14.4	-24.5	4.0	-15.6

**TABLE 3** Sensitivity test results: the % change in concentrations of  $C_6-C_{10}$  aldehydes in the apartment in Milan for typical summer conditions relative to baseline conditions

in deposition velocities are clearly key factors for model output. For instance, under baseline conditions, 26% of ozone deposition is to the walls, but this becomes 63% for the 75th percentile run and affects the resulting aldehyde concentration mix. Yields of hexanal and heptanal are reported to be very low from painted walls<sup>14,63</sup>; therefore, increasing the rate of ozone deposition to walls does not lead to any increase in their concentrations. As Figure 2 shows, the median deposition velocity value is closer to the 25th percentile for some surfaces and 75th for others, reflecting the large range of values currently existing in the literature.

The age of the surface also affects the aldehyde yields, which in turn affects aldehyde production rates and concentrations. Table 1 shows that the relatively few measurements of aldehyde yields from walls suggest rates are higher from older materials. Consequently, in the sensitivity tests in Table 3, some aldehyde concentrations are higher for new materials, while others are higher for older materials compared to the baseline. Clearly, far more information about these

parameters in real-world environments would reduce model uncertainties considerably.

The model predictions are less sensitive to the photolysis, outdoor  $NO_x$  concentrations, and variation of HMIX. For instance, increasing photolysis rates based on the upper bounds of transmitted light through windows<sup>42</sup> increases the predicted aldehyde concentrations by ~30%-36%. However, either the increase or decrease of HMIX by 50% changes the  $C_6-C_{10}$  concentrations by only 5%-10%. Doubling or halving outdoor  $NO_x$  concentrations decreased or increased, respectively, the concentrations of  $C_6-C_{10}$  aldehydes by ~15%.

These sensitivity tests provide an estimate of the likely range of the model indoor aldehyde concentrations given the uncertainties in the input values. Clearly, the largest source of uncertainty in the model output is driven by the uncertainty in the deposition velocities. As we tested model sensitivity to the 25th and 75th percentile values of this parameter, we estimate the uncertainties in the model estimates of

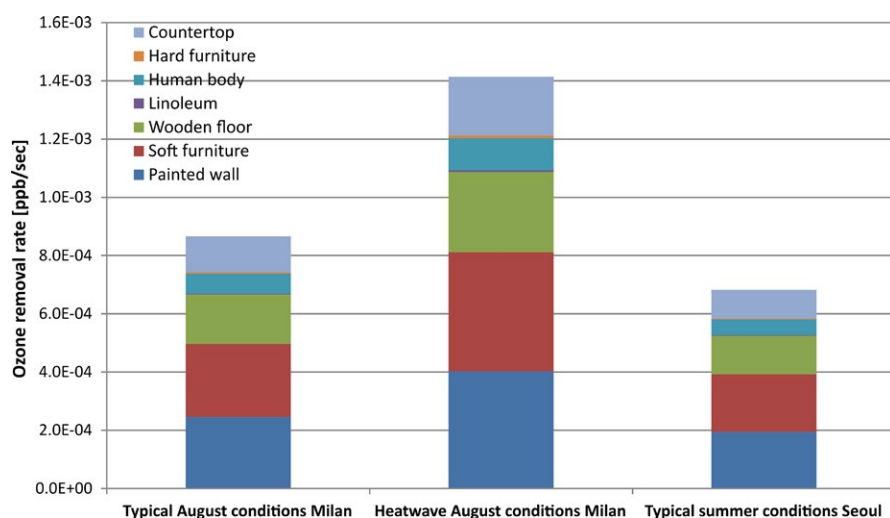


**FIGURE 3** Total ozone removal rate [ppb/s] onto different indoor surfaces (average age) in the Milan apartment during typical and heatwave conditions and in the Seoul apartment during typical summer time conditions



aldehyde concentrations to be approximately double the sensitivity reported to the deposition velocities in Table 3, so 80%-100%.

### 3.2 | Ozone surface deposition

The model results show that approximately 85% of the indoor ozone is deposited onto internal materials for both typical and heatwave conditions (note that model inputs are the same for the three runs except for outdoor ozone and  $\text{NO}_x$  concentrations). However, different types of surface are more effective ozone sinks than others as shown in Figure 3.

The deposition velocities presented in Figure 2 show that human bodies, carpets, and soft furniture are expected to be the most reactive materials for the indoor environment with linoleum and hard furniture the least. Indeed, the highest loss rate per square meter is to human bodies for all three sets of conditions. Although the surface-volume ratio of the human body is the lowest ( $0.03 \text{ m}^{-1}$ ) for all surfaces in the apartment, the ozone deposition velocity is the highest (Figure 2). However, in terms of total ozone deposition to each surface, most is deposited on the painted wall and ceilings and to the soft furnishings (both around 30% of the total), compared to the human body (~8%) owing to the larger available area of the former two surfaces.

### 3.3 | Surface production

#### 3.3.1 | Production from indoor materials

The average production rates of  $\text{C}_6\text{-C}_{10}$  aldehydes following surface interactions of ozone with different surfaces have been investigated as discussed in the Methods section. Note that although we investigated the impact of human skin emissions on the total  $\text{C}_6\text{-C}_{10}$  aldehyde mixing ratios in the apartment, they were very low (~0.1 ppb for nonanal and ~0.2 ppb for decanal) for our assumed conditions and we have excluded them from Figure 4. The concentrations of

aldehydes formed following ozone deposition were analyzed for typical conditions in Milan and categorized by surface (Figure 4). For comparison, Figure 4 also shows the predicted nonanal concentrations for the heatwave conditions in Milan as well as summer conditions for Seoul, given it was the most important contributor to the total  $\text{C}_6\text{-C}_{10}$  concentration.

Painted walls, due to having the largest surface-volume ratio, made the biggest contribution to indoor nonanal and decanal concentrations, with countertops and soft furniture also providing a significant fraction of the total given the high yields presented in Table 1. For hexanal, secondary emissions from wooden floors were most important.

There are very few studies with which to compare our predictions of  $\text{C}_6\text{-C}_{10}$  aldehydes indoors and they are perhaps not directly comparable. However, our results are in reasonable agreement with a study that reports measured values in ~4000 Canadian households,<sup>58</sup> though tend to be on the higher end of the measured ranges (75th-99th percentile) except for hexanal which is closer to the geometric mean. Likewise, both Reiss et al.<sup>64</sup> and Marchand et al.<sup>1</sup> report mean hexanal mixing ratios of ~2 ppb hexanal, while Liu et al.<sup>65,66</sup> report mean mixing ratios of closer to 1 ppb. For nonanal, our values are relatively high compared to the measurements of Zhu et al.,<sup>58</sup> who report a 99th percentile value of ~2.5 ppb. However, the painted walls make a significant contribution to our predicted concentrations and the yield values used are based on relatively few measurements. Clearly, the assumptions made about the surfaces in our apartment compared to those that existed in real buildings where measurements were made will be significant in any comparison. While our predicted values appear to be representative of magnitudes observed, there is a clear need for more measurements to help validate models results.

#### 3.3.2 | Production from skin surface

The results we have considered so far are whole apartment average values. Within this context, emissions of pollutants from two

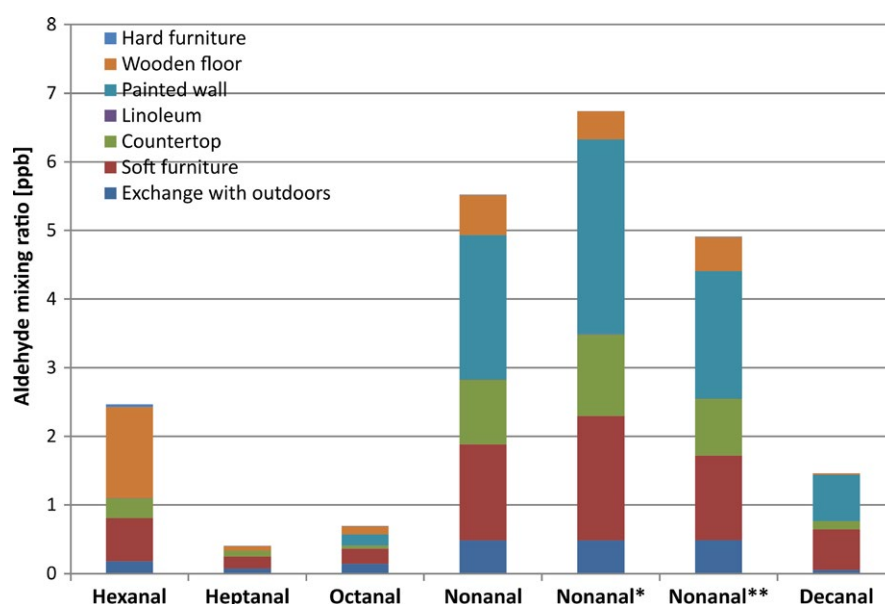


**FIGURE 4**  $\text{C}_6\text{-C}_{10}$  aldehyde mixing ratios indoors following ozone surface deposition in the Milan apartment for typical summer conditions (\*in the Milan apartment for extreme summer conditions; \*\*in the Seoul apartment for typical summer conditions)



or three human occupants would be relatively small assuming a well-mixed environment. For instance, the presence of three people in the apartment for typical Milan summer conditions enhances the nonanal and decanal mixing ratios by only  $\sim 0.1$  and  $\sim 0.2$  ppb, respectively. Therefore, to estimate the impact when human emissions can be more important, we investigated the indoor air quality for an occupied bedroom at nighttime and for different ventilation rates (Figure 5). We assumed that two adults (surface estimated as  $4 \text{ m}^2$  in total;  $\text{HMIX}=0.22 \text{ m}^{-1}$ ) were in the room ( $7.5 \text{ m}^3$ ) continuously for 8 hours (23:00–07:00 hours). The internal surfaces included soft furniture ( $5 \text{ m}^2$ ;  $\text{HMIX}=0.28 \text{ m}^{-1}$ ), painted walls and ceiling ( $30.6 \text{ m}^2$ ;  $\text{HMIX}=1.7 \text{ m}^{-1}$ ), wooden floor ( $7.5 \text{ m}^2$ ;  $\text{HMIX}=0.42 \text{ m}^{-1}$ ), and hard furniture ( $6.3 \text{ m}^2$ ;  $\text{HMIX}=0.35 \text{ m}^{-1}$ ). The total surface to volume ratio is  $\sim 2.96 \text{ m}^{-1}$ . The volume of the bedroom was  $18 \text{ m}^3$  so emissions into this smaller volume were adjusted accordingly, while external conditions were kept the same as described in the Methods.

We focused on human skin oxidation-derived emissions of higher aldehyde species already included in the model mechanism (nonanal, decanal, 4-OPA) and with yields as reported in Table 1, although we appreciate this list is not exhaustive. For instance, geranyl acetone and 6-methyl-5-hepten-2-one (6-MHO) have both been reported as species that are emitted from skin,<sup>22</sup> but degradation schemes for these two products are not currently available in the MCM. Note that the indoor nighttime ozone was in the range of 0.6–4 ppb indoors at nighttime (dependent on air exchange rate), significantly lower than the daytime values.

Figure 5 shows carbonyl concentrations decrease at lower AERs, given less ozone is transported indoors under these conditions to drive the surface interactions. 4-OPA and decanal are the most important of the studied species, but only attain mixing ratios of up to 1 ppb: The nonanal concentration is typically  $\sim 60\%$  of the value of the other two. Given that nonanal and decanal are emitted both from surface materials and from human skin interactions, their importance can be compared. For an AER of 0.76 per hour, the nonanal mixing ratio estimated from emissions from internal materials was 3.7 ppb and for decanal 1.2 ppb. This is compared to concentrations of 0.5 ppb of nonanal and 0.7 ppb

of decanal from skin for the same AER. Note that in the absence of human occupants, the nonanal and decanal concentrations are reduced by  $\sim 0.1$  ppb each. Although the human occupants are responsible for more than 0.1 ppb of the total concentrations shown in Figure 5, in their absence, there is more deposition to other surfaces, from which secondary emissions are less efficient. So for these aldehyde species and under these conditions, ozone-driven emissions from furniture and building materials generate higher concentrations than those from humans. Our predictions are in good agreement with the measurements of Järnström et al.,<sup>67</sup> who measured mean annual concentrations of around 1.2 and 0.8 ppb of nonanal and decanal, respectively, in bedrooms of 12-month-old Finnish homes with a mean AER of 0.9 per hour.

### 3.4 | Impacts of oxidation-derived surface emissions on chemical processing indoors

Most of the discussion has focused on ozone deposition and the production of aldehydes within the studied buildings. Here, the INDCM is used to investigate whether the oxidation-derived emissions of these aldehydes also have an impact on the chemical processing. In order to understand exactly how the chemistry changes when the oxidative production of these aldehydes are included, compared to when they are absent, and the implications for formation of other secondary pollutants, a rate of production analysis was carried out for the Milan apartment during typical summertime conditions (Figure 6).

The modeled steady-state concentrations of OH,  $\text{HO}_2$ , and  $\text{RO}_2$  for a model run with ozone deposition only (no emissions) were  $4.8 \times 10^5 \text{ mol cm}^{-3}$  and 4.9 and 6.0 ppt, respectively. With surface production included, the same concentrations were  $3.7 \times 10^5 \text{ mol cm}^{-3}$  and 4.0 and 5.5 ppt, respectively. Considering the radical initiation processes first, production of  $\text{HO}_2$  radicals via photolysis of aldehydes increases significantly when ozone-derived surface aldehyde emissions and hence concentrations increase. Initiation rates of radical formation via  $\text{O}_3$ -terpene reactions remain similar with or without ozone-driven production of aldehydes on surfaces, but photolysis of dicarbonyl species becomes less important with the emissions. Dicarbonyls are

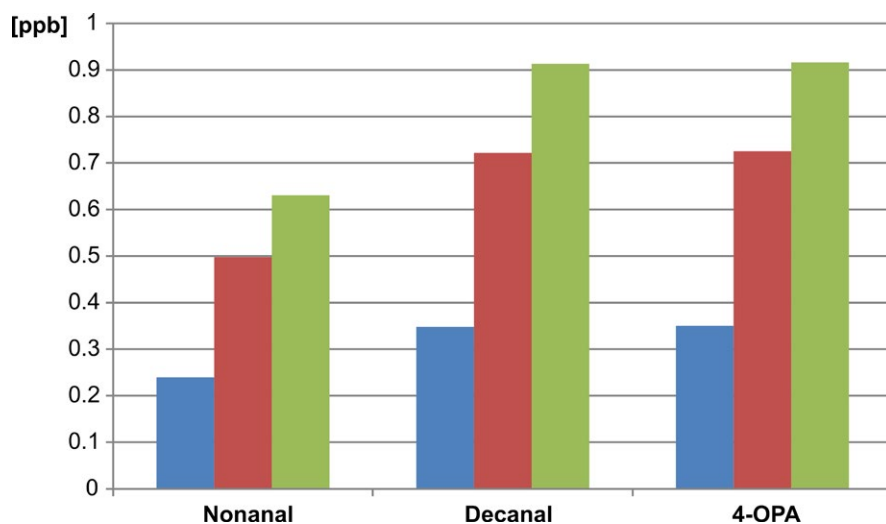


**FIGURE 5** Mixing ratios of selected aldehydes indoors following ozone deposition to human skin in a bedroom in the Milan apartment for typical nighttime summer conditions. Note that blue bars depict mixing ratios of the aldehydes when air exchange rate is  $0.2 \text{ h}^{-1}$ , red bars  $0.76 \text{ h}^{-1}$ , green bars  $2.0 \text{ h}^{-1}$

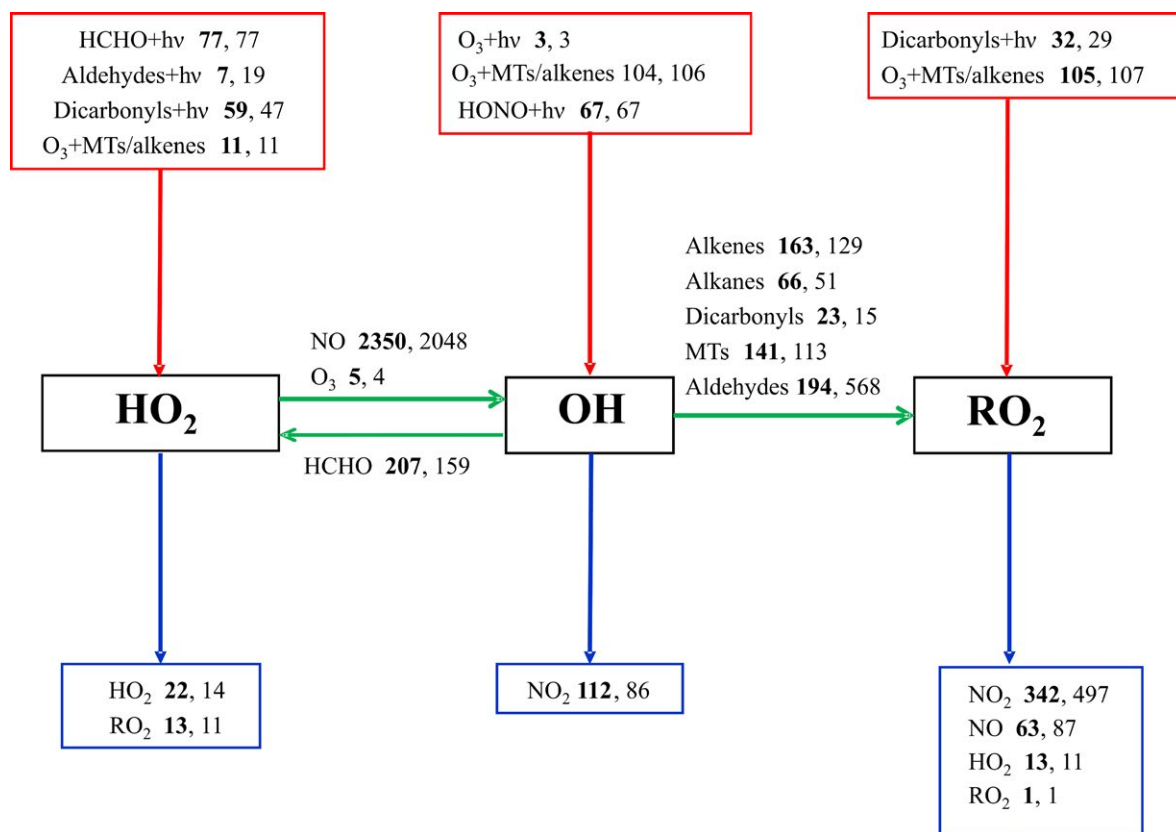


**FIGURE 6** Rate of production analysis for the major rates of reaction for a model run with ozone deposition and no oxidation-derived aldehyde emissions (figures in bold) and with ozone deposition followed by ozone-driven aldehyde surface production (normal font) in units of  $10^4 \text{ mol cm}^{-3} \text{ s}^{-1}$ . MT denotes monoterpene. Red arrows denote radical initiation processes, and blue arrows are termination processes with green arrows representing radical propagation. Note that RO<sub>2</sub> includes RCO<sub>3</sub> acetyl-type peroxy radicals (eg, CH<sub>3</sub>CO<sub>3</sub>) as well as alkyl peroxy radicals, RO<sub>2</sub> (eg, CH<sub>3</sub>O<sub>2</sub>)

formed in numerous places in the model mechanism, such as through OH attack on alcohol species. The concentration of OH decreases by about 23% when oxidative production of aldehydes on surfaces is included, and hence, formation of dicarbonyls is also suppressed.

In terms of radical propagation, increased aldehyde concentrations enable a higher production rate of acetyl peroxy radicals via reaction with OH, which more than offsets the decreased formation rate of peroxy radicals from other processes when oxidation-derived aldehyde emissions are considered. Perhaps the most interesting difference is when one considers the fate of the peroxy radicals through termination processes. Reactions of alkyl peroxy radicals with NO to form organic nitrates and of acetyl peroxy radicals with NO<sub>2</sub> to form PAN-type species dominate RO<sub>2</sub> loss whether ozone-driven aldehyde emissions are considered or not. The proportion of acetyl relative to alkyl peroxy radicals increases with higher aldehyde concentrations enhancing faster formation of PAN-type species. The overall concentration of RO<sub>2</sub> is similar for both scenarios, but the changed composition shifts the termination processes toward formation of the nitrated organic species. Interestingly, Weschler et al.<sup>22</sup> found that the concentration of organic nitrates and PAN-type species increased by—a factor of 2 when soiled tee shirts were introduced into an aircraft cabin with ozone, compared to when they were absent. Therefore, an important implication of surface processing indoors is that we may expect to find

more nitrated organic species compared to the situation where there is no oxidative production of aldehydes on surfaces.

We carried out a similar analysis to investigate the impact of humans on indoor air chemistry in the bedroom as described above (not shown). We noted very similar effects, namely increased importance of aldehydes and the enhanced formation of nitrated organic carbon species. Weschler<sup>68</sup> suggested that the presence of humans in a building would decrease the net level of oxidants. The results from the INDCM confirm this finding. It is well known that the ozone is deposited onto skin and other surfaces indoors. However, our results also confirm that the OH radical concentration is decreased as ozone-driven surface emissions are included in the model, owing to the higher concentrations of aldehyde species.

## 4 | CONCLUSIONS

In this study, we compared the surface interactions for typical furnished apartments for different outdoor pollution levels and in different locations. Not surprisingly, high outdoor ozone concentrations can enhance indoor air pollution and lead to higher emissions of C<sub>6</sub>-C<sub>10</sub> aldehydes. For instance, concentrations of nonanal increased by ~22% during polluted conditions when compared with more average

conditions in Milan. Given that heat waves may become more frequent in future with climate change,<sup>69</sup> indoor ozone-derived surface aldehyde emissions may also increase.

Among all the tested surfaces, the human body was shown to be the most efficient in terms of removing ozone from indoor air per square meter. However, when internal ozone-driven emissions of aldehydes are considered, soft furniture and painted walls become more important owing to their larger surface areas in a typical building. Ozone-initiated emissions from the human body can be important in smaller areas of a house (eg, a bedroom at nighttime), when concentrations of various carbonyl species can become significant. An important conclusion from our study is that inclusion of oxidation-derived surface emissions (from surfaces and/or people) within a detailed chemical model profoundly affects chemical processing. Ozone-driven surface emissions deplete oxidants, increase the importance of radical production from aldehyde photolysis indoors, and shift formation of products toward nitrated organic carbon species.

Even though indoor surfaces can be quite different in their initial reactivity, aging and soiling of surfaces may make indoor surfaces more similar than different over time.<sup>70</sup> In a study of five homes, Wang and Morrison<sup>38</sup> showed that older carpet was less reactive than new carpet, but that kitchen countertops tended to remain reactive regardless of age and that this was probably due to continuous application of cooking oils and/or cleaning agents. Occupants also add to the reactivity of surfaces via desquamation (skin shedding) and transferring skin oils to surfaces.<sup>68</sup> This process of slow oxidation of the original surfaces (or surface films) and continuous deposition of reactive organic material may result in indoor surfaces, especially upward-facing horizontal surfaces, having similar chemical properties. Therefore, models will benefit from more extensive field measurements of ozone surface reactivity (deposition velocity and product yields) in occupied homes, as well as information on surface interactions for indoor pollutants other than ozone.

## ACKNOWLEDGEMENTS

This research is part of Cutting-edge Approaches for Pollution Assessment in Cities (CAPACITIE) project, which has received funding from the European Union's Seventh Framework Programme for research, technological development, and demonstration under grant agreement no 608014. We would like to acknowledge the help of Charlie Weschler with interpretation of the yield data for emissions of aldehydes from skin.

## REFERENCES

1. Marchand C, Bulliot B, Le Calvé S, Mirabel Ph. Aldehyde measurements in indoor environments in Strasbourg (France). *Atmos Environ*. 2006;40:1336-1345.
2. Lee SC, Li WM, Ao CH. Investigation of indoor air quality at residential homes in Hong Kong—case study. *Atmos Environ*. 2002;36:225-237.
3. Lin HH, Ezzati M, Murray M. Tobacco smoke, indoor air pollution and tuberculosis: a systematic review and meta-analysis. *PLoS Med*. 2007;4:173-189.
4. Wolkoff P, Schneider T, Kildesø J, Degerth R, Jaroszewski M, Schunk H. Risk in cleaning: chemical and physical exposure. *Sci Total Environ*. 1998;215:135-156.
5. Coleman BK, Destailats H, Hodgson AT, Nazaroff WW. Ozone consumption and volatile byproduct formation from surface reactions with aircraft cabin materials and clothing fabrics. *Atmos Environ*. 2008;42:642-654.
6. Clausen PA, Wilkins CK, Nielsen GD. Formation of strong airway irritants in terpene/ozone mixtures. *Indoor Air*. 2000;10:82-91.
7. Nazaroff WW, Weschler CJ. Cleaning products and air fresheners: exposure to primary and secondary air pollutants. *Atmos Environ*. 2004;38:2841-2865.
8. Morrison GC. Recent advances in indoor chemistry. *Curr Sust Renew Energy Rep*. 2015;2:33-40.
9. Reiss R, Ryan PB, Koutrakis P. Modeling ozone deposition onto indoor residential surfaces. *Environ Sci Technol*. 1994;28:504-513.
10. Fischer A, Ljungström E, Langer S. Ozone removal by occupants in a classroom. *Atmos Environ*. 2013;81:11-17.
11. Weschler CJ. Ozone in indoor environments: concentration and chemistry. *Indoor Air*. 2000;10:269-288.
12. Lin CC, Hsu SC. Deposition velocities and impact of physical properties on ozone removal for building materials. *Atmos Environ*. 2015;101:194-199.
13. Kim S, Kim JA, Kim HJ, Do Kim S. Determination of formaldehyde and TVOC emission factor from wood-based composites by small chamber method. *Polym Test*. 2006;25:605-614.
14. Wang H, Morrison GC. Ozone-initiated secondary emission rates of aldehydes from indoor surfaces in four homes. *Environ Sci Technol*. 2006;40:5263-5268.
15. Morrison GC, Nazaroff WW. The rate of ozone uptake on carpets: experimental studies. *Environ Sci Technol*. 2000;34:4963-4968.
16. Cox SS, Little JC, Hodgson AT. Predicting the emission rate of volatile organic compounds from vinyl flooring. *Environ Sci Technol*. 2002;36:709-714.
17. Wilke O, Jann O, Brödner D. VOC- and SVOC-emissions from adhesives, floor coverings and complete floor structures. *Indoor Air*. 2004;14:98-107.
18. Hodgson AT, Beal D, McIlvaine JER. Sources of formaldehyde, other aldehydes and terpenes in a new manufactured house. *Indoor Air*. 2002;12:235-242.
19. Waring MS, Siegel JA. Indoor secondary organic aerosol formation initiated from reactions between ozone and surface-sorbed d-Limonene. *Environ Sci Technol*. 2013;47:6341-6348.
20. Mendell MJ. Indoor residential chemical emission as risk factors for respiratory and allergic effects in children: a review. *Indoor Air*. 2007;17:259-277.
21. Wisthaler A, Weschler CJ. Reactions of ozone with human skin lipids: Sources of carbonyls, dicarbonyls, and hydroxycarbonyls in indoor air. *PNAS*. 2010;107:6568-6575.
22. Weschler CJ, Wisthaler A, Cowlin S, et al. Ozone-initiated chemistry in an occupied simulated aircraft cabin. *Environ Sci Technol*. 2007;41:6177-6184.
23. Mochalski P, King J, Unterkofler K, Hinterhuber H, Amann A. Emission rates of selected volatile organic compounds from skin of healthy volunteers. *J Chromatogr B*. 2014;959:62-70.
24. Carslaw N. A new detailed chemical model for indoor air pollution. *Atmos Environ*. 2007;41:1164-1179.
25. Carslaw N, Mota T, Jenkin ME, Barley MH, McFiggans G. A significant role for nitrate and peroxide groups on indoor secondary organic aerosol. *Environ Sci Technol*. 2012;46:9290-9298.
26. Jenkin ME, Saunders SM, Pilling MJ. The tropospheric degradation of volatile organic compounds: a protocol for mechanism development. *Atmos Environ*. 1997;31:81-104.
27. Jenkin ME. Modelling the formation and composition of secondary organic aerosol from  $\alpha$ - and  $\beta$ -pinene ozonolysis using MCM v3. *Atmos Chem Phys*. 2004;4:1741-1757.

28. Saunders SM, Jenkin ME, Derwent RG, Pilling MJ. Protocol for the development of the master chemical mechanism, MCM v3 (part A): tropospheric degradation of non-aromatic volatile organic compounds. *Atmos Chem Phys*. 2003;3:161-180.
29. Bloss C, Wagner V, Jenkin ME, et al. Development of a detailed chemical mechanism (MCMv3.1) for the atmospheric oxidation of aromatic hydrocarbons. *Atmos Chem Phys*. 2005;5:641-664.
30. Morrison GC, Nazaroff WW. Ozone interactions with carpet: secondary emissions of aldehydes. *Environ Sci Technol*. 2002;36:2185-2192.
31. Grontoft T, Raychaudhuri MR. Compilation of tables of surface deposition velocities for O<sub>3</sub>, NO<sub>2</sub> and SO<sub>2</sub> to a range of indoor surfaces. *Atmos Environ*. 2004;38:533-544.
32. Klenø JG, Clausen PA, Weschler CJ, Wolkoff P. Determination of ozone removal rates by selected building products using the FLEC emission cell. *Environ Sci Technol*. 2001;35:2548-2553.
33. Nicolas M, Ramalho O, Maupetit F. Reactions between ozone and building products: impact on primary and secondary emissions. *Atmos Environ*. 2007;41:3129-3138.
34. Sabersky RH, Sinema DA, Shair FH. Concentrations, decay rates, and removal of ozone and their relation to establishing clean indoor air. *Environ Sci Technol*. 1973;7:347-353.
35. Tamás G, Weschler CJ, Bakó-Biró Z, Wyon DP, Strøm-Tejsten P. Factors affecting ozone removal rates in a simulated aircraft cabin environment. *Atmos Environ*. 2006;40:6122-6133.
36. Poppendieck D, Hubbard H, Ward M, Weschler CJ, Corsi RL. Ozone reactions with indoor materials during building disinfection. *Atmos Environ*. 2007;41:3166-3176.
37. Hoang CP, Kinney KA, Corsi RL. Ozone removal by green building materials. *Build Environ*. 2009;44:1627-1633.
38. Wang H, Morrison GC. Ozone-surface reactions in five homes: surface reaction probabilities, aldehyde yields, and trends. *Indoor Air*. 2010;20:224-234.
39. Gall ET, Darling E, Siegel JA, Morrison GC, Corsi RL. Evaluation of three common green building materials for ozone removal, and primary and secondary emissions of aldehydes. *Atmos Environ*. 2013;77:910-918.
40. Rim D, Gall ET, Maddalena RL, Nazaroff WW. Ozone reaction with interior building materials: influence of diurnal ozone variation, temperature and humidity. *Atmos Environ*. 2016;125:15-23.
41. Gall ET, Siegel JA, Corsi RL. Modeling ozone removal to indoor materials, including the effects of porosity, pore diameter, and thickness. *Environ Sci Technol*. 2015;49:4398-4406.
42. Drakou G, Zerefos C, Ziomas I, Voyatzaki M. Measurements and numerical simulations of indoor O<sub>3</sub> and NO<sub>x</sub> in two different cases. *Atmos Environ*. 1998;32:595-610.
43. Abbass OA, Sailor DJ, Gall ET. Effect of fiber material on ozone removal and carbonyl production from carpets. *Atmos Environ*. 2017;148:42-48.
44. Chacon-Madrid HJ, Presto AA, Donahue NM. Functionalization vs. fragmentation: n-aldehyde oxidation mechanisms and secondary organic aerosol formation. *Phys Chem Chem Phys*. 2010;12:13975-13982.
45. Bowman JH, Barket DJ, Shepson PB. Atmospheric chemistry of nonanal. *Environ Sci Technol*. 2003;37:2218-2225.
46. Terry AC, Carslaw N, Ashmore M, Dimitroulopoulou S, Carslaw DC. Occupant exposure to indoor air pollutants in modern European offices: an integrated modelling approach. *Atmos Environ*. 2014;82:9-16.
47. Sangiorgi G, Ferrero L, Ferrini BS, et al. Indoor airborne particle sources and semi-volatile partitioning effect of outdoor fine PM in offices. *Atmos Environ*. 2013;65:205-214.
48. Carslaw N, Ashmore M, Terry AC, Carslaw DC. Crucial role for outdoor chemistry in ultrafine particle formation in modern office buildings. *Environ Sci Technol*. 2015;49:11011-11018.
49. The CAPACITIE project. <https://www.york.ac.uk/yes/projects/capacitie/>. Accessed January, 2017.
50. Tae S, Shin S, Woo J, Roh S. The development of apartment house life cycle CO<sub>2</sub> simple assessment system using standard apartment houses of South Korea. *Renew Sust Energy Rev*. 2011;15:1454-1467.
51. Singer BC, Hodgson AT, Hotchi T, et al. Sorption of organic gases in residential rooms. *Atmos Environ*. 2007;41:3251-3265.
52. Cuéllar-Franca RM, Azapagic A. Environmental impacts of the UK residential sector: life cycle assessment of houses. *Build Environ*. 2012;54:86-99.
53. Murray DM, Burmaster DE. Residential air exchange rates in the United States: empirical and estimated parametric distributions by season and climatic region. *Risk Anal*. 1995;15:459-465.
54. Dimitroulopoulou C. Ventilation in European dwellings: a review. *Build Environ*. 2012;47:109-125.
55. EU AirBase. <http://www.eea.europa.eu/data-and-maps/data/air-base-the-european-air-quality-database-3>. Accessed October, 2016.
56. The EU OFFICAIR project. <http://www.officair-project.eu/>. Accessed October, 2016.
57. Sarwar G, Corsi RL, Kimura Y, Allen D, Weschler CJ. Hydroxyl radicals in indoor environments. *Atmos Environ*. 2002;36:3973-3988.
58. Zhu J, Wong SL, Cakmak S. Nationally representative levels of selected volatile organic compounds in Canadian residential indoor air: population-based survey. *Environ Sci Technol*. 2013;47:13276-13283.
59. Gandolfo A, Gligorovski V, Bartolomei V, et al. Spectrally resolved actinic flux and photolysis frequencies of key species within an indoor environment. *Build Environ*. 2016;109:50-57.
60. Nazaroff WW, Cass GR. Mathematical modelling of chemically reactive pollutants in indoor air. *Environ Sci Technol*. 1986;20:924-934.
61. IUPAC. Task group on atmospheric chemical kinetic data evaluation. 2016. <http://www.iupac-kinetic.ch.cam.ac.uk/>. Accessed June, 2016.
62. Carslaw N, Jacobs PJ, Pilling MJ. Modeling OH, HO<sub>2</sub>, and RO<sub>2</sub> radicals in the marine boundary layer: 2. Mechanism reduction and uncertainty analysis. *J Geophys Res*. 1999;104:30257-30273.
63. Lamble SP, Corsi RL, Morrison GC. Ozone deposition velocities, reaction probabilities and product yields for green building materials. *Atmos Environ*. 2011;45:6965-6972.
64. Reiss R, Ryan PB, Tibbetts SJ, Koutrakis P. Measurement of organic acids, aldehydes, and ketones in residential environments and their relation to ozone. *J Air Waste Manag Assoc*. 1995;45:811-822.
65. Liu W, Zhang J, Zhang L, et al. Estimating contributions of indoor and outdoor sources to indoor carbonyl concentrations in three urban areas of the United States. *Atmos Environ*. 2006;40:2202-2214.
66. Liu W, Zhang JJ, Korn LR, et al. Predicting personal exposure to airborne carbonyls using residential measurements and time/activity data. *Atmos Environ*. 2007;41:5280-5288.
67. Järnström H, Saarela K, Kalliokoski PE, Pasanen AL. Reference values for indoor air pollutant concentrations in new, residential buildings in Finland. *Atmos Environ*. 2006;40:7178-7191.
68. Weschler CJ. Roles of the human occupant in indoor chemistry. *Indoor Air*. 2016;26:6-24.
69. Solomon S, Qin D, Manning M, et al. *Contribution of Working Group I to the Fourth Assessment Report of the Intergovernmental Panel on Climate Change, 2007*. Cambridge, United Kingdom and New York, N.Y.: Cambridge University Press; 2007.
70. Nazaroff WW, Gadgil AJ, Weschler CJ. Critique of the use of deposition velocity in modeling indoor air quality. In: Nagda NL, ed. *Modeling of Indoor Air Quality and Exposure*. Philadelphia, PA: ASTM STP 1205; 1993:81-104.

**How to cite this article:** Kruza M, Lewis AC, Morrison GC, Carslaw N. Impact of surface ozone interactions on indoor air chemistry: A modeling study. *Indoor Air*. 2017;00:1-11. <https://doi.org/10.1111/ina.12381>